Electronic Supplementary Material (ESI) for Lab on a Chip.

Supplementary Information

Patterned Microfluidic Devices for Rapid Screening of Metal-Organic Frameworks Yields Insights into Polymorphism and Non-Monotonic Growth

Paria Coliaie[1], Rajan Bhawnani[1], Aditya Prajapati[1], Rabia Ali[1], Prince Verma[2], Gaurav Giri[2], Manish S. Kelkar[3], Akshay Korde[3], Marianne Langston[4], Chengxiang Liu[5], Neda Nazemifard[4], Daniel Patience[6], Tamar Rosenbaum[7], Dimitri Skliar[8], Nandkishor K. Nere[1,3], and Meenesh R. Singh[1]*

[1]Department of Chemical Engineering, University of Illinois at Chicago, Chicago, IL 60607
[2]Department of Chemical Engineering, University of Virginia, Charlottesville, Virginia 22903, United States
[3]Center of Excellence for Isolation & Separation Technologies (CoExIST), Process R&D, AbbVie Inc., North Chicago, IL 60064
[4]Pharmaceutics Research – Analytical Development, Takeda Pharmaceuticals International Co., Cambridge, MA 02139
[5]Pharmaceutical Development, Biogen, Cambridge, MA 02142
[6]Chemical Process Development, Biogen, Cambridge, MA 02142
[7]Bristol-Myers Squibb Co., Drug Product Science & Technology, New Brunswick, NJ 08901
[8]Bristol Myers Squibb Co., Chemical & Synthetic Development, New Brunswick NJ 08901

Corresponding Author:
Prof. Meenesh R. Singh
Assistant Professor
Department of Chemical Engineering
929 W. Taylor St.
University of Illinois at Chicago
Chicago, IL 60607
Tel: (312) 996-3424
Email: mrsingh@uic.edu

Keywords: Metal-organic framework, Polymorphism, MOF screening, Patterned microfluidics, growth rate

Table of Contents

S1 Dimensions of the Patterned-Surface Microfluidic Device

The dimension of the patterned surfaces is shown in Figures S1 and S2. Figure S1 and S2 show the density of patterns and height for the $100\mu m$ and $200\mu m$ size patterns, respectively. The list of these dimensions is provided in Table S1 and S2. These pattern surfaces are attached to the microfluidic mixer device with open top and bottom surfaces. In Figure S3, the microfluidic mixer device with open sides is shown. The dimensions of the design parameters are also shown in Figure S3.

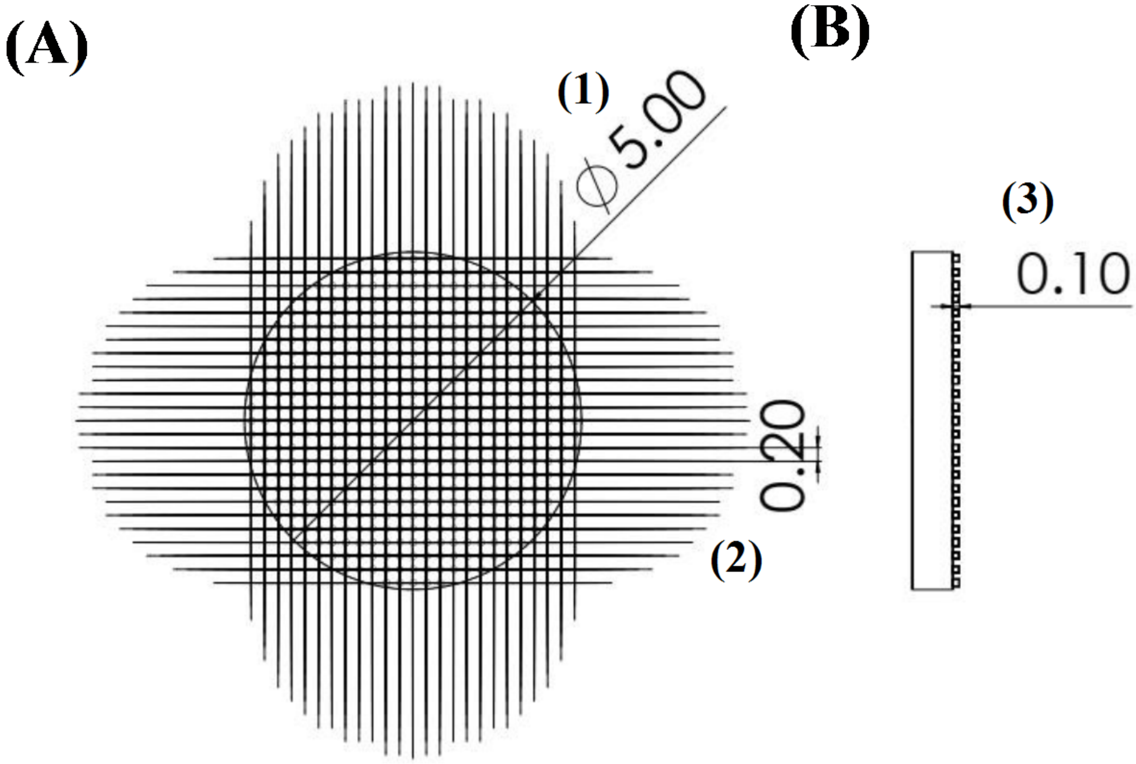

Figure S1: (A) Top view and **(B)** side view of the $100\mu m$ size patterned surface with marked dimensions.

Table S1: List of the dimensions of the $100\mu m$ size patterned surface with marked dimensions.

Feature	**Size (mm)**
(1) Diameter of the patterned Surface	5
(2) Center to center distance of patterns	0.2
(3) Height of the patterns	0.1

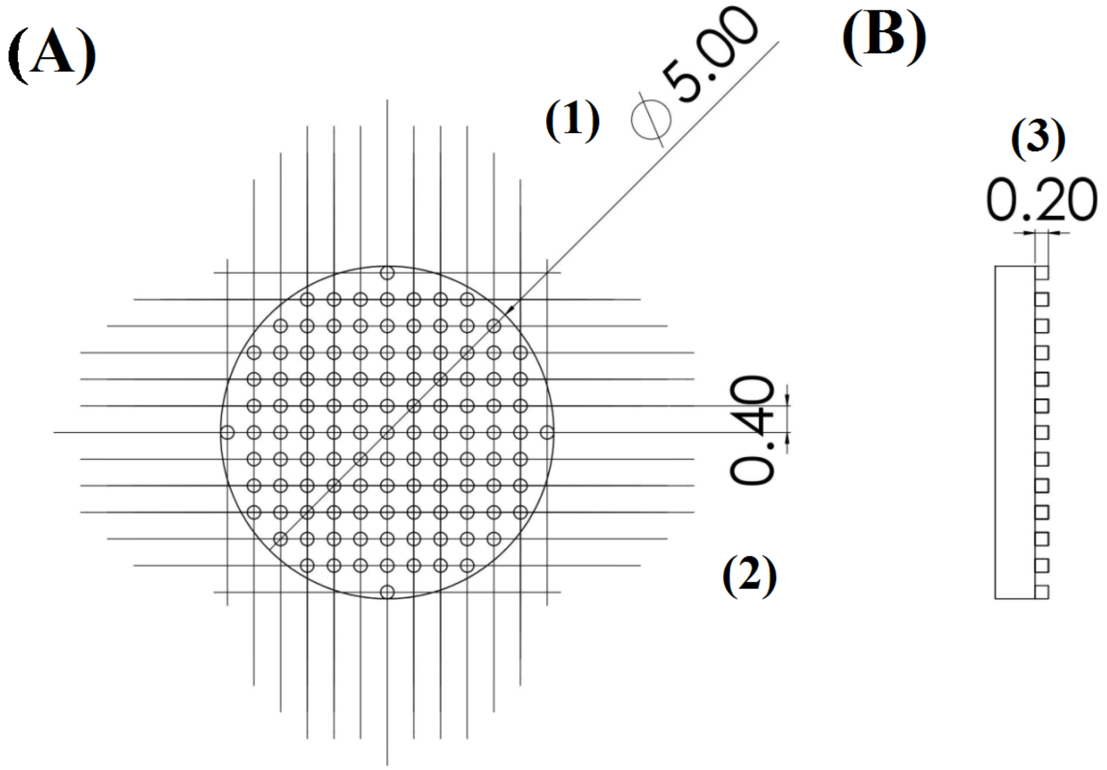

Figure S2: **(A)** Top view and **(B)** side view of the 200μm size patterned surface with marked dimensions.

Table S2: List of the dimensions of the 200μm size patterned surface with marked dimensions.

Feature	**Size** (mm)
(1) Diameter of the patterned Surface	5
(2) Center to center distance of patterns	0.4
(3) Height of the patterns	0.2

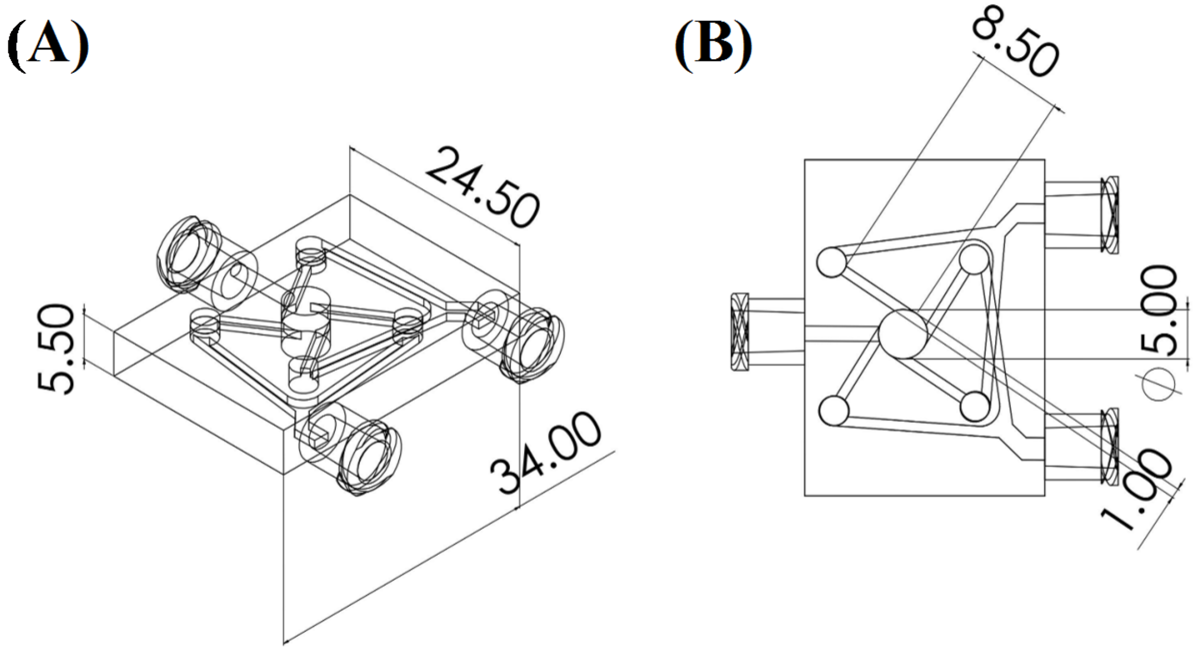

Figure S3: (A) Isometric view and **(B)** top view of the microfluidic mixer device with open top and bottom side with marked dimensions.

S2 COMSOL Simulation of the Patterned-Surface Microfluidic Device

S2.1 Laminar Flow Module: Equations and Boundary Conditions

The laminar flow module of COMSOL was used to calculate the velocity profile in the microfluidic mixer. The time-dependent Navier stock equation solved is described as follows:

$$\rho\frac{\partial u}{\partial t}+\rho(u.\nabla)u=\nabla.[-p.I+\mu(\nabla u+(\nabla u)^{T})+F \qquad \text{Eq (1)}$$

Where ρ and μ are density and the viscosity of water which is assumed to be incompressible. Here the selected boundary conditions for the patterned surface microfluidic device are shown below. Figure S4 shows the isometric view of the imported 3D file of the jacketed microfluidic mixer device in the COMOSL Multiphysics for the simulation. In Figure S2B, the assigned boundary conditions for this system are shown and listed as:

Boundary Conditions:

→ Inlet $_{1,\ \mathrm{Mixer}}$ = Inlet $_{2,\ \mathrm{Mixer}}$: $Q_{Mixer} = 0.5\ mL.min^{-1}$
→ Outlet $_{\mathrm{Mixer}}$: $P = 1\ atm$

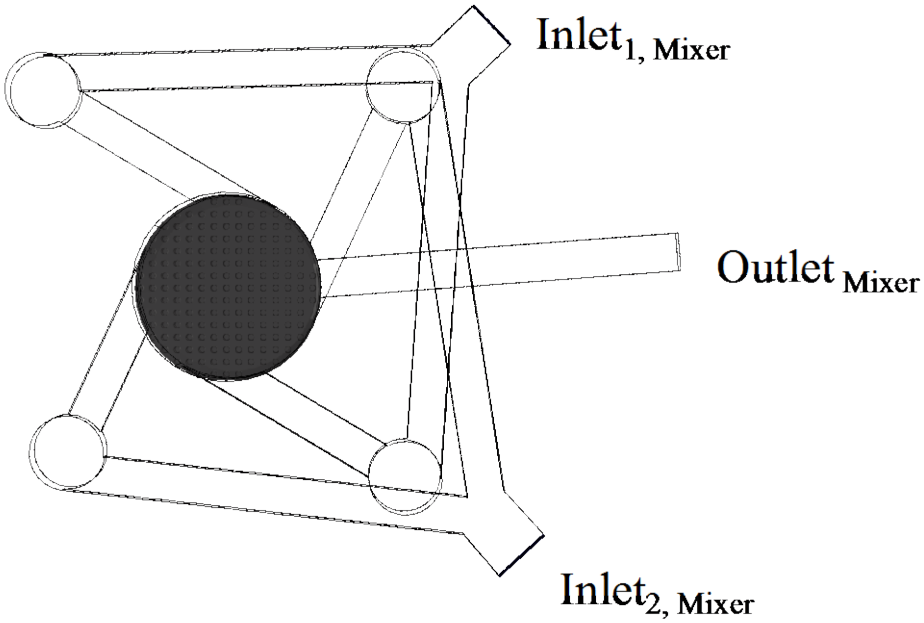

Figure S4: The top view of the patterned-surface microfluidic mixer device with the assigned boundary conditions for the mixer. (Patterns are located on the bottom surface)

S2.2 Transport of Diluted Species Module: Equations and Boundary Conditions

The transport of the diluted species module is used to calculate the concentration profile in the microfluidic mixer. The time-dependent continuity equation solved is described as follows:

$$\rho \frac{\partial c_i}{\partial t} + \nabla.(-\mathrm{D_i}\nabla \mathrm{c_i}) + u.\nabla \mathrm{c_i} = \mathrm{R_i} \qquad \text{Eq (2)}$$

which includes both convection and diffusion for the transport mechanisms. Here ρ is the density, and u is the velocity of the fluid and comes from the laminar flow module. These two modules are coupled together, and the velocity profile is directly substituted into the continuity equation. The assigned boundary conditions for this model are listed below:

Boundary Conditions:

- → Inlet $_{1,\ \text{Mixer}}$: $c_i = c_{0,i} = 0\ mol.m^{-3}$
- → Inlet $_{2,\ \text{Mixer}}$: $c_i = c_{0,i} = 1\ mol.m^{-3}$
- → Outlet $_{\text{Mixer}}$: $n.D_i \nabla c_i = 0$

S2.3 Model Parameters of the COMSOL Simulations

This study simulates a coupled analysis of the laminar flow module and mass transfer in diluted species to evaluate the velocity, pressure, and concentration profile inside the patterned surface microfluidic mixer. The 3D model for simulations was imported into the model from a SolidWorks design. The design was further simplified by eliminating the sharp edges and smoothening the surfaces to enhance the mesh quality. The free tetrahedral mesh was selected for the models. The tetrahedral mesh was selected for this study, and the details are provided in the following part:

- Maximum Element Size = 1.15 mm
- Minimum Element Size = 0.207 mm
- Maximum Element Growth Rate = 1.5

- Curvature Factor = 0.6
- Resolution of Narrow Region = 0.5

The coupled equations of the Navier stock and mass balance were solved in the stationary solver using “PARADISO” solver. The residual tolerance was set to 0.01 with 100 iterations and left preconditioning. Newton was selected as the non-linear method with a damping factor of 0.1 and tolerance as the termination technique. The relative tolerance was also kept at 0.001. The temperature-dependent viscosity and density of the water were considered in the model.

S3 Fabrication of the Patterned-Surface Microfluidic Device

The microfluidic devices were fabricated using stereolithography (SLA) 3D printing technology. First, the CAD design of the microfluidic devices is prepared with SolidWorks® (2020, Dassault Systems), and then a commercial 3D printer (form 3, Formlabs Inc., USA) is used to print the microfluidic devices. The selected resin for the prints was the clear resin which is chemically resistant to various solvents, including ethanol and water. After printing the device, they are washed in an isopropyl alcohol (IPA) (90%, Sigma-Aldrich) bath for 20 mins in the Form Wash (Formlabs Inc., USA) to remove the residues of the resin from the external surface. Next, the interior channels of the 3D printed device were washed separately by injecting IPA using a syringe to eliminate the uncured residues of the resin in the channels.

As shown in Figure 1A in the manuscript, the top and bottom faces of the microfluidic mixer were kept open to maximize optical clarity. The open holes on both sides were sealed with polycarbonate films using a fresh, clear resin. First, the area around the circular zone is covered with fresh uncured resin (from the resin tank), and a polycarbonate film is put on that. Next, the device is cured under UV light for 10 minutes to seal the open area.

S4 Experimental Details

S4.1 Experimental Details for Screening the Effect of Solvent

Details of the precursor solutions for samples A and B are listed in Table S3. The molar ratio of the Copper Nitrate Trihydrate to Trimesic acid is kept at 1.5 for both solvents. Thus, for each sample, a total volume of 50 ml of the precursors. For sample A, both precursors are dissolved in ethanol, and for sample B, copper nitrate is dissolved in water and Trimesic acid in the ethanol.

Table S3: Details for the precursor solutions for the effect of the solvent experiments

Sample	Cu/TA (mol)	Solvents
A	1.5	Both solvents Ethanol
B	1.5	Ethanol: Water (0.3:1)

S4.2 Experimental Details for Screening the Effect of pH

Details for the precursor solutions for the sample with no additive, with acidic, and with basic modulators are listed in Table S4. The neutral sample is sample A, and acetic acid and pyridine are used as the acidic and basic modulators. Ten mol equivalents to TA of acetic acid (acid modulator) and pyridine (Basic modulators) were added to the organic linker solution (Trimesic acid in ethanol) in the respective studies.

Table S4: Details for the precursor solutions for the effect of the pH

Sample	Cu/TA (mol)	Solvents	Modulator
Acidic	1.5	Both solvents Ethanol	Acetic Acid
Neutral	1.5	Both solvents Ethanol	-
Basic	1.5	Both solvents Ethanol	Pyridine

S4.2.1 Effect of pyridine on the HKUST-1 crystals

The modulators used in this study are used as capping agents for crystal growth. Using FT-IR, we have confirmed that the addition of pyridine does not affect the chemistry of the HKUST-1 crystals.

In-situ FT-IR studies were performed on a Bruker Invenio-S spectrometer in attenuated total reflectance (ATR) mode using a Pike VeeMax-III ATR module. A Ge crystal fixed on a steel base was placed on the ATR accessory. A Jackfish spectroscopic well was mounted on the surface of the crystal. The spectra at each timestamp were recorded with a spectral resolution of 2 cm^{-1} at a low sampling rate of 7.5kHz. The beam aperture was set to 6 mm, and the specular angle was set to 60 degrees.

Study 1: *Monitoring pyridine concentration in HKUST-1 solution after pyridine addition over 30 minutes.*

In this study, the spectra of HKUST-1 in ethanol were recorded. First, the background was subtracted using that solution prior to the addition of pyridine. Then, pyridine of concentration equal to the amount used in the effect of pH studies was added to the reaction mixture, and the spectra were monitored for 30 minutes. The pyridine spectral intensities did not change throughout this experiment (see Figure S5). In this figure, the negative absorbances are an artifact of the background-subtracted solution.

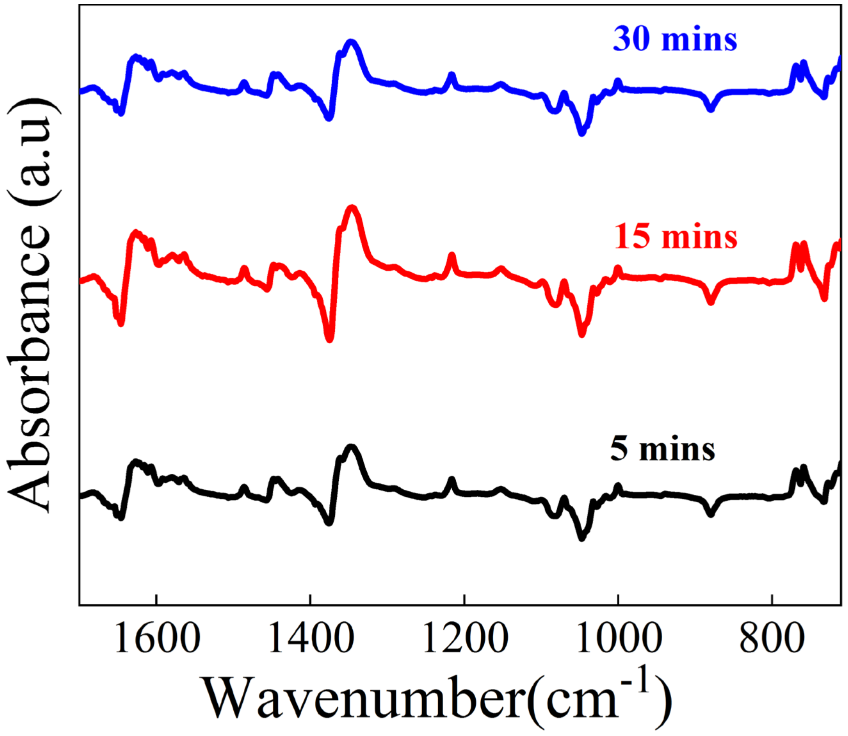

Study 2: *Monitoring HKUST-1 spectra after pyridine addition*.

In this study, the background was subtracted with ethanol only, and HKUST-1 solution spectra were recorded at time t=0 minutes. Pyridine was then added, and the spectra were monitored for about 30 minutes. Additional peaks after pyridine addition appeared (barely significant), but the signature HKUST-1 spectral peaks remain unaffected.

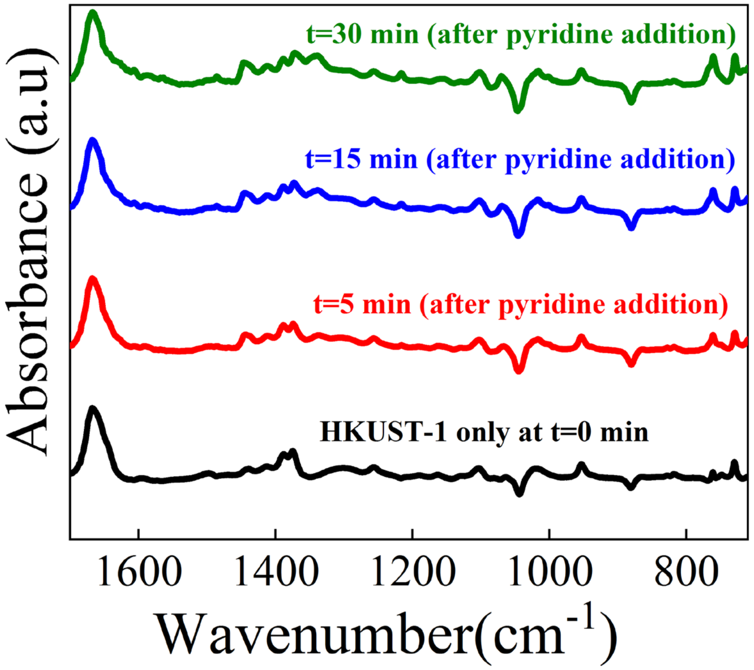

These two studies show that pyridine is neither consumed nor affects the chemical structure of HKUST-1. Moreover, identical P-XRD spectra (in the absence and presence of the basic modulator) shown in Figure 4E also provide evidence that the overall crystal structure remains unaltered.

It is possible that the presence of basic modulators alters the speciation during the pre-crystallization phase of the reaction. It has been hypothesized from previous studies that a basic environment leads to faster deprotonation during speciation, which further enhances nucleation. However, since the time scale of this pre-crystallization phase is in the order of nano- to microseconds, it is difficult to lay down the exact mechanism of speciation using FT-IR. It can be concluded that these modulators act as capping agents that reduce the average particle size and narrower distributions without affecting the final chemical structure of the product.

S4.3 Area Enhancement Factor for the Patterned Surface Microfluidic Devices

The presence of the patterns on the bottom side of the device increases the existing surface area for the heterogeneous reaction. Here the enhanced area is calculated and divided by the area of the bottom surface when no pattern exists. This ratio is called Area Enhancement Factor and is measured for all six patterns. Here $N_{Pattern}$ is the total number of patterns.

$$Area\ Enhancment\ Factor = F_{AE} = \frac{N_{Pattern} \times (\pi D_{Pattern} L + 2\frac{\pi D_{Mixer}^2}{4})}{\frac{\pi D_{Mixer}^2}{4}}$$

Using this equation, the area enhancement factor is calculated for the circular patterns with 0.1 and 0.2 μm diameters and height.

Circular Patter with a diameter of 100 μm:

$$F_{AE} = Area\ Enhancment\ Factor = \frac{646 \times (\pi \times 0.1 \times 0.1 + \frac{0.1^2}{2})}{\frac{\pi \times 5^2}{4}} = 1.55$$

Circular Patter with a diameter of 200 μm:

$$F_{AE} = Area\ Enhancment\ Factor = \frac{113 \times (\pi \times 0.2 \times 0.2 + \frac{0.2^2}{2})}{\frac{\pi \times 5^2}{4}} = 1.0848$$

In Table S5, we have listed the area enhancement factor for all six patterns.

Table S5: Area Enhancement factor for all six patterned surfaces

Pattern Shape	Inscribed Circle Diameter (mm)	F_{AE}
Circular	0.1	1.6
Circular	0.2	1.1
Squared	0.1	1.9
Squared	0.2	1.3
Hexagonal	0.1	1.9
Hexagonal	0.2	1.3

S5 BET Surface area characterization

The porosity of the synthesized HKUST-1 crystals was determined by recording the nitrogen (N_2) adsorption-desorption isotherms at 77 K (**Figure S7a**). The HKUST-1 crystals exhibit type I isotherm[1], as expected since HKUST-1 only contains micropores. Additionally, the steep uptake at the low-pressure region indicates the presence of large micropore volumes. The calculated Brunauer–Emmett–Teller (BET) surface area of the HKUST-1 is 893 m^2/g which is on the same order of magnitude as reported in the literature.[2,3] Furthermore, the pore size distribution (**Figure S7b**) demonstrates the presence of smaller pores (aperture = 9.5 Å) of HKUST-1 crystals. The larger pores (aperture = 14 Å) of HKUST-1 crystals could not be captured during pore size analysis due to the unavailability of enough data points at the low-pressure region.

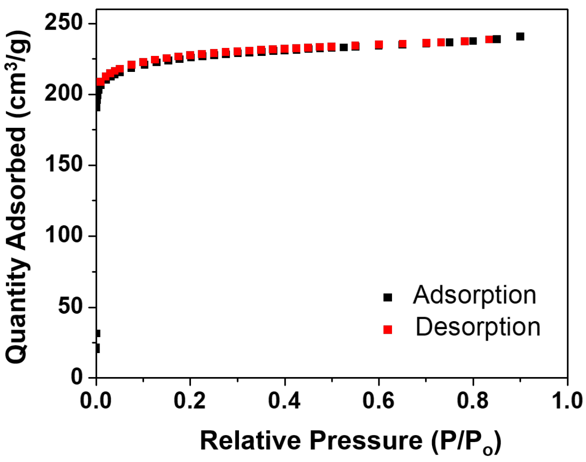

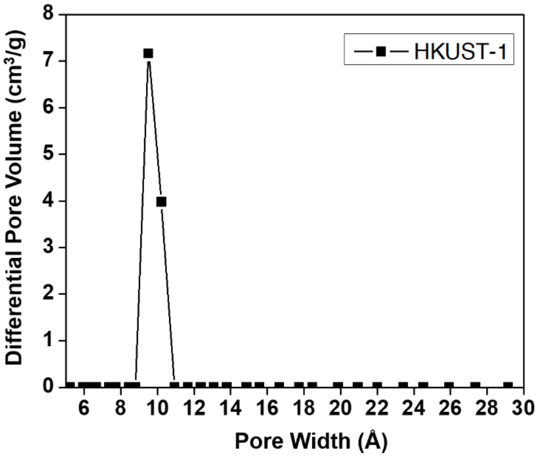

Fig S7: (a) N_2 adsorption-desorption isotherms of the synthesized HKUST-1 crystals in the continuous microfluidic mixer using ethanol as solvent in both the precursors. (b) Pore size distribution of the synthesized HKUST-1 crystals

References

1. Ambroz, F.; Macdonald, T. J.; Martis, V.; Parkin, I. P. Evaluation of the BET theory for the characterization of meso and microporous MOFs. *Small Methods* **2018**, 2, No. 1800173.
2. Vrtovec, N.; Mazaj, M.; Buscarino, G.; Terracina, A.; Agnello, S.; Arčon, I.; Kovač, J.; Logar, N. J. Structural and CO2 capture properties of ethylenediamine-modified HKUST-1 metal-organic framework *Cryst. Growth Des.* **2020**, 20, 5455–5465.
3. Chuah, C. Y.; Goh, K.; Bae, T.-H. Hierarchically structured HKUST-1 nanocrystals for enhanced SF6 capture and recovery. *J. Phys. Chem. C* **2017**, 121, 6748−6755.